Journal of Porous Materials (2019) 26:1755–1765
https://doi.org/10.1007/s10934-019-00757-3

Water-glass based silica aerogel: unique nanostructured filler for epoxy nanocomposites

S. Salimian[1] · **A. Zadhoush**[1]

Published online: 6 June 2019

Abstract
Due to the unique properties such as 3-dimensional nanoporous structure and high surface area, silica aerogel is a promising candidate for replacing the conventional micron-sized silica to improve the mechanical properties of epoxy-based nanocomposites. In the present study, the water-glass based silica aerogel was first synthesized by the low-cost sodium silicate and cheap ambient pressure drying method and then used as the filler in the epoxy system. Finally, rheological and mechanical properties of the silica aerogel-epoxy nanocomposite were investigated. The introduction of silica aerogel powders impacted the rheological properties of epoxy dispersion and improved the mechanical performance of the corresponding nanocomposite. The dispersion microstructure has been characterized by its rheological properties and has been used to determine the critical silica aerogel weight fraction of the network formation (φ*) for the silica aerogel-epoxy dispersion. At the critical filler concentrations (φ*), the overall mobility of the polymer chains is restricted in both dispersion and solid nanocomposites. Therefore, the network structure and the interface surrounding nanoparticles increases and this results in an improvement of the mechanical properties. Mechanical tests showed improvements in flexural modulus and strength by ~ 80% and ~ 40% respectively as compared with those of pure epoxy. Based on this study, water-glass based silica aerogel hold great promise as a low-cost filler in polymer composite.

Keywords Silica aerogel · Polymer nanocomposite · Rheology · Interface

1 Introduction

Silica aerogels are highly crosslinked and porous materials that consist of more than 90% nanoporous matrices and less than 10% amorphous silica particles that are interconnected [1–3]. This results in a material with low density (~ 0.003–0.5 g cm^{-3}), low thermal conductivity [0.005–0.1 W/(mK)], ultra-low dielectric constant (k = 1.0–2.0) and low index of refraction (~ 1.05) [4, 5]. These unusual characteristics of aerogel have led to its use in various industrial applications such as thermal insulation materials [6, 7], heat storage devices [8], and acoustic barrier materials [9]. However, widespread applications of silica aerogel have been restricted because of their extreme fragility and poor mechanical properties [10]. Therefore, to overcome the fragility, different methods have been explored to improve the mechanical properties of silica aerogels such as hybridization of silica aerogels with different polymeric systems [11, 12], or incorporation of various fibrous supporting materials into the aerogel systems [13, 14]. A new approach is proposed by Du et al. [15], wherein the use of aerogel is considered as a filler into resins in order to improve the mechanical and thermal properties of the resins. This approach refers to nanoparticle/matrix polymer composites in which the mesopores are completely filled with the polymers [16, 17].

Improvements in performance of composites in terms of strength, modulus, fracture toughness and thermal stability are accomplished by introducing nanoparticles as fillers in polymers [18, 19]. Silica nanoparticles [20, 21], carbon nano tubes (CNTs) [22, 23], metal oxides (e.g. SiO_2, TiO_2, Al_2O_3, and Fe_3O_4) [24, 25] and layered silicates (e.g. montmorillonite) [26, 27], are the most common dopant in use as a filler in polymers. Despite the wide array of nanoparticles available for composite preparation, two issues continually interfere with optimal composite performance: (1) aggregation and (2) the lack of a strong interaction between the polymer

✉ S. Salimian
s.salimian@alumni.iut.ac.ir

[1] Department of Textile Engineering, Isfahan University of Technology, Isfahan 84156-83111, Iran

matrix and filler [28, 29]. Introducing of mesoporous silica as filler in polymer composites has generated great interest due to its potential to tackle the difficulties of both aggregation and interfacial interaction [30–32]. Interest in mesoporous fillers is boosted by the inability of polymer chains to effectively impregnate microporous fillers which lead to increases the interfacial interaction and adhesion between the polymer components and the inorganic fillers [33, 34].

Nowadays, silica aerogel materials have attracted considerable interests in applications of reinforcing agent for the preparation of new structured polymer composite materials due to their large pore sizes, high specific surface area and mesoporosity [35]. It has been showed that by adding these mesoporous materials into polymer matrix, the fracture toughness (K_{Ic}) and energy (G_{Ic}) properties, tensile strength, storage and loss modulus, thermal stability and glass transition temperature (Tg) have been greatly improved [36, 37]. Zhao et al. and Gupta et al. demonstrated that the silica aerogel pore are infiltrated by resin [38, 39]. According to Maghsoudi et al. aerogel/epoxy composites have remarkable toughness and yielding behaviors compared to neat epoxy, with its brittle behavior. In another work, Halim et al. obtained good thermal and mechanical properties for unsaturated polyester (UP) composite filled with silica aerogel with preserved pores. Their study also showed that the dispersion of PVA-coated aerogel with preserved pores in the polyester matrix resulted in an increase of specific compressive strength, thermal insulation and thermal stability [40]. Recently, Kaya et al. presented the silica xerogel/epoxy nanocomposites with uniform dispersion of silica xerogel in epoxy matrix. Their results showed that the presence of silica xerogel resulted in a nanocomposite with high thermal stability and low thermal conductivity [41]. The significant improvement in the properties of the silica aerogel filled polymer composites is directly related to the extremely light and loosely packed structure of aerogel results in excellent dispersion of interconnected silica nanoparticles in the matrix without any need for surface modification, co-solvents, or surfactants [42]. Additionally, other kind of aerogel such as carbon and graphene aerogel were also investigated as a potential candidate for reinforcing polymer composite [43, 44].

Epoxy resins have been widely mounted in various field of application such as electronic devices, sealants, paints, coatings and adhesives, due to their good mechanical stability, superior electric isolation, easy handling, and low cost [45, 46]. However, epoxy resin suffer from the relatively poor toughness and poor resistance to crack propagation [47, 48]. Therefore, the incorporation of appropriate reinforcement and filler in epoxy matrix are required.

In this study, low cost silica aerogel was easily synthesized from water-glass as a precursor and cheap ambient pressure drying method to be used as filler in epoxy nanocomposites for the first time. We have investigated dispersions and solid nanocomposites of water-glass based silica aerogel in epoxy to estimate the reinforcement effects of silica aerogel. We stress the rheological characterization of low and high concentrated silica aerogel-epoxy dispersions to evaluate the transition of the structure from viscous liquid to elastic solid behavior. Furthermore, the mechanical properties of solid composites are investigated with respect to the dispersion microstructure, fracture analysis and interface properties.

2 Experimental

2.1 Materials

This epoxy resin used was a standard diglycidyl ether of bis-phenol A (DGEBA) with an epoxide equivalent weight (EEW) of 185 g/eq., 'LY556' supplied by Huntsman, UK. The curing agent is a polyetheramine (trade name of Jeffamine T-403) supplied by Huntsman with a nominal amine group content of 6.1 to 6.6 mol/kg.

2.2 Synthesizing of silica aerogel

The silica wet gel was prepared with a water-glass or sodium silicate solution (FAMCO, Iran) as starting materials. The sodium silicate solution was diluted to 1:4 (V/V) with water and then, went through an ion exchange column (8 cm in diameter, 40 cm in length) filled with 1 L of Amberlite IR 120 H ion exchange resin-filled column. The collected silicic acid had the pH values of 2.4–2.7. For gelation, 1.0 M ammonia solution was added to the collected silicic acid to adjust the pH values from 3.5 to 4.5. After gelation, the wet gels were aged for 3 h in deionized water to strengthen their gel structure and then, were immersed in the propone-2-ol, *n*-Hexane, and TMCS/*n*-Hexane (1:5 V/V) mixture for 24 h to be changed to alcogel, organogel, and modified-organogel, respectively. The schematic procedure for fabricating the silica aerogel is shown in Fig. 1. The surface modified gels were dried at room temperature and then heat-treated at 80 °C and then 200 °C for 2 h to reduce shrinkage during drying and complete the evaporation of the pore liquid. This procedure was used according to the previous study by Mazrouei et al. [49].

2.3 Preparation of silica aerogel-epoxy dispersion

Epoxy resin dispersions were prepared by incorporating 1, 2 and 4 wt% of the silica aerogel into the liquid epoxy resin, respectively. High-speed (600 rpm) mechanical stirring was then performed at room temperature followed by sonification

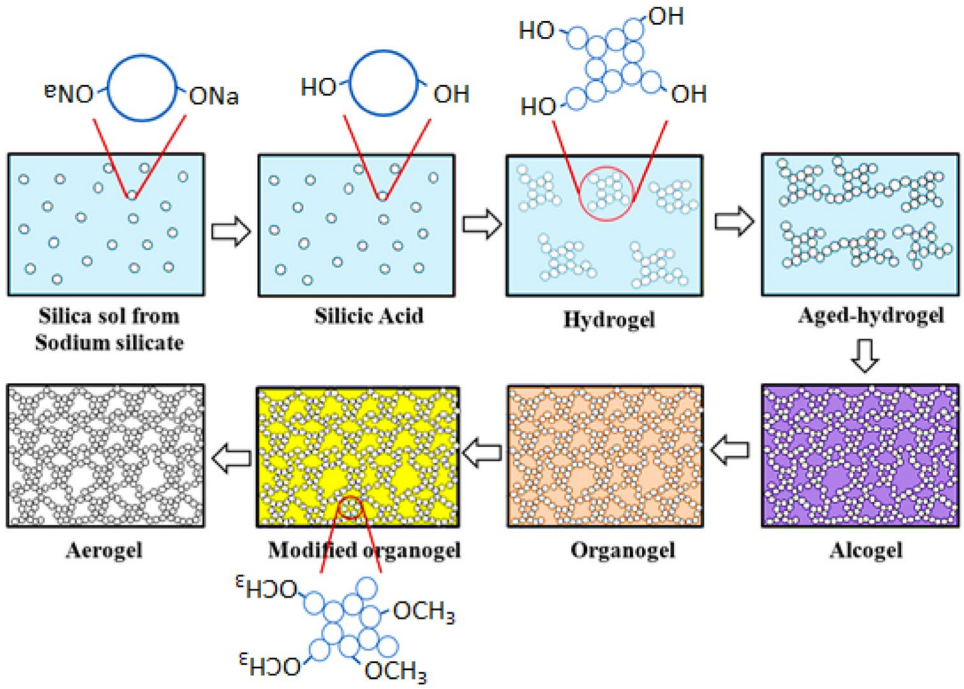

Fig. 1 A schematic of aerogel synthesizing

for 15 min at room temperature. Samples of solid composites were prepared as polyetheramine in stoichiometric proportions, 40 parts per hundred parts of DGEBA resin (phr), was added to the dispersions as a hardener according to the stoichiometric ratio given by the manufacturer, and they were cured for 1 h at room temperature which was followed by post-curing for 3 h at 140 °C. A schematic illustration of the sample preparation is shown in Fig. 2.

2.4 Characterization

The mesoporous structure of silica aerogel examined by N_2 adsorption–desorption isotherm with TriStar II plus (USA) at 77 K. Before measurements, the sample was pretreated for 6 h at 423 K and 0.3 kPa. The specific surface area was calculated by the Brunauer–Emmett–Teller (BET) method while pore size was obtained from the Barrett–Joyner–Halenda (BJH) model.

IR spectra of silica aerogel powders were recorded on a Hartmann and Braun spectrometer (Canada) equipped with a universal ATR sampling accessory to investigate the surface functionalities of silica aerogel.

For Transmission electron microscopy (TEM) tests, specimens were cut off the nanocomposite using an ultramicrotome (REICHERT-JUNG ULTRACUT E MICROTOME WITH STEREO STAR ZOOM 0.7 ×–4.2 × 570) equipped with a diamond knife (DiATOME Diamond Knives, ultra 35°) to a thickness about 70–90 nm. Thin specimens were

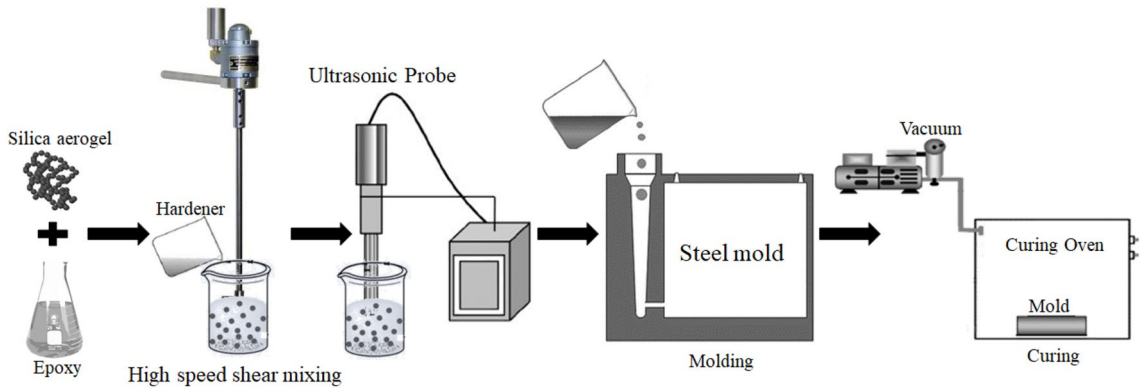

Fig. 2 Schematic illustration of the fabrication of silica aerogel/epoxy nanocomposite. With permission of Ref. [36]

also cut from a mesa of about 1×1 mm^2. The samples were attached on a 300 mesh copper grids (PLANO-Multipacks, S162-3-V, Formvar/carbon on 300 mesh copper). TEM images were taken on a JEOL JEM-100CX II microscope at an accelerating voltage of 120 kV.

The rheological characteristics of the silica aerogel-epoxy dispersions were measured with AR 2000ex Rheometer with cone–plate geometry. The oscillatory shear mode in the frequency range of 0.1–100 s^{-1} at a low strain amplitude of 0.01% was used to measure the dynamic storage modulus (G′) and loss modulus (G″) within the linear viscoelastic range.

Dynamic mechanical analysis (Q800 V20.8 Build 26) was carried out at a fixed frequency of 1 Hz to obtain values of Tan (δ) and the storage modulus (E′).

Compression and flexural tests were carried out using Universal Testing System Z010 (Zwick, Germany), according to ASTM D695 [50] and ASTM D790 [51], respectively.

The dispersion quality of the silica aerogel in the resin is monitored by SEM ((Philips XL30) with acceleration voltage of 20 kV.

3 Results

3.1 Silica aerogel characterization

The N_2 adsorption isotherm of the mesoporous silica aerogel is typical of type IV with a hysteresis loops at P/P0 > 0.5 indicative of mesopores structure according to the IUPAC classification [52] as shown in Fig. 3a. The specific surface area, pore volume and average pore size of silica aerogel are 810 m^2/g, 3 cm^3/g and 10 nm respectively. The microstructure of silica aerogel is shown by FE-SEM photos in Fig. 3c. The image clearly demonstrate the homogeneous silica network with porous structure. Silica aerogel network are schematically illustrated in Fig. 3c. It can be seen that, the aerogel structure are loosely stacked which leads to decreased van de Waals interactions and makes the powders readily redispersed in appropriate media. There are already some works reported that the excellent dispersion of silica in the matrix led to nanocomposites, which display a significant mechanical reinforcement when compared to the neat polymer [53, 54]. Good dispersability of the silica in the polymer is a prerequisite to create polymer/silica aerogel nanocomposites that display a significant mechanical reinforcement [55].

ATR-FTIR spectra of silica aerogel powder are shown in Fig. 3b. The dominant peaks observed at 1256 and 846 cm^{-1} correspond to Si–C bonds representative of tetramethylsilane

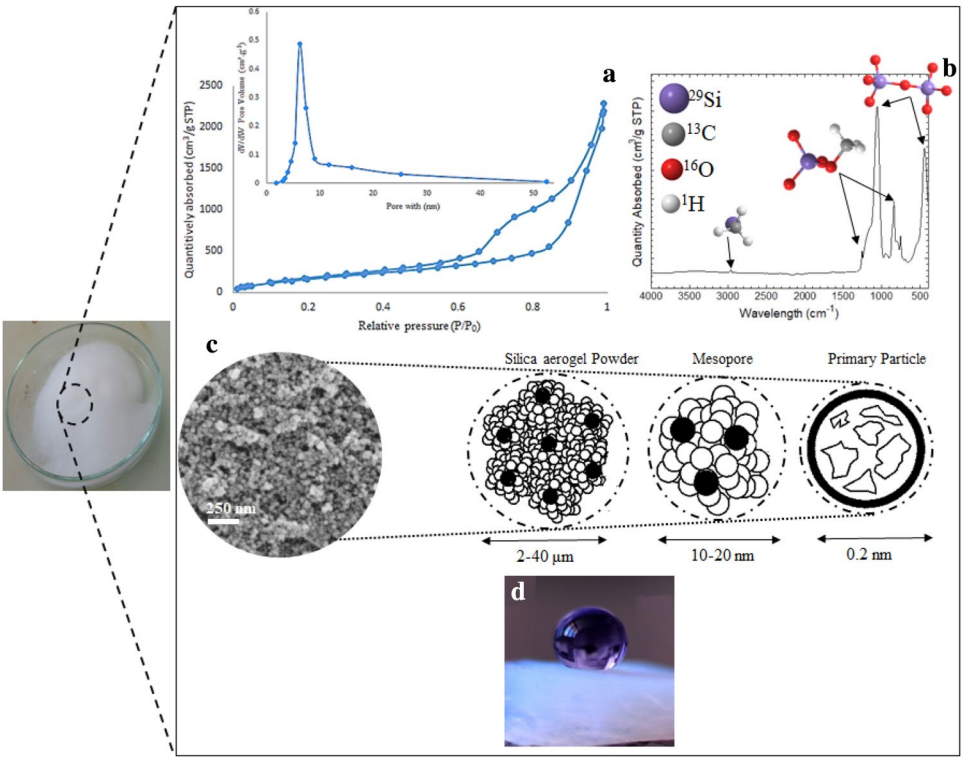

Fig. 3 **a** N_2 adsorption–desorption isotherms (inset: pore size distributions), **b** ATR-FTIR spectra, **c** FE-SEM images and **d** water contact angle of hydrophobic mesoporous silica aerogel

(TMS) in hydrophobic silica aerogels [56]. The strong peak at 1085 cm^{-1} and weaker peak at 450 cm^{-1} are corresponding to stretching vibrations of Si–O–Si bond [57]. The absence of peaks near 3430 (absorption of –OH) and 1645 cm^{-1} (bending of H–O–H) are due to substitution of hydrophilic groups with hydrophobic TMS groups. In addition, apart from Si–O–Si and Si–C peaks, the absorption peaks at 2963 corresponding to $–CH_3$ terminal groups are visible which consistent with the surface modification of the silica aerogel by TMCS [58]. Moreover, the aerogel granules exhibit a high water contact angle of 150°, Fig. 3d, which is attributed to the silica aerogel surface modified by the TMCS hydrophobic agent.

3.2 Rheological properties of the silica aerogel-epoxy dispersions

Figure 4a–c shows the storage modulus (G′, elastic property) and loss modulus (G′, viscous property) as a function of frequency and silica aerogel loading. Both G′ and G″ increase significantly with an increase of the silica aerogel loading. However, the rate of increase becomes slower in the dispersion with higher silica aerogel loadings. The silica aerogel loading is observed to have more impact on the modulus at low frequencies than that at high ones. When the silica aerogel loading is above 2 wt%, G′ is observed to be almost independent of the frequency which could be related to the formation of a network structure. It is shown that the structural network is constructed by the intimate contact of the fillers which are wrapped with the absorbed polymer [59, 60]. By increasing the filler content, an inter-connected network structure is formed at a critical filler loading (φ*) which is regarded as a rheological percolation concentration. The rheological properties of such percolated dispersions are changed at φ*. Below φ*, dispersions are weakly shear-thinning and show little or no viscoelasticity while beyond φ*, solid-like behavior is observed [61]. A schematic model of percolated network formations are depicted in Fig. 4a″–c″). The crossing point of the G′ and G″ indicates a switch from viscous liquid to elastic solid behavior [42]. According to Fig. 4a–c, the crossing points of dispersion with 1, 2 and 4 wt% of silica aerogel are observed at 0.7, 70 and 90 s^{-1} respectively. Therefore, the dispersion with silica aerogel content of φ* experience an earlier transition from viscous to elastic state. In addition, the SiO_2 distributions in the epoxy matrix are investigated using the SEM–EDX mapping technique, Fig. 4a′–c′. The white points in the EDX images denote Si atoms. It is worthy to note that an increased viscoelastic properties (G′ > G″) with an improved dispersion quality by increasing silica aerogel content is observed and is due to the increased physical confinement of polymer chains in mesopores of silica aerogel. These observations can be ascribed to the formation of an interface layer consisting of entangled polymers inside the aerogel pores, which results in an improvement of the compatibility between the silica aerogel and epoxy polymer. Recently, a new model of

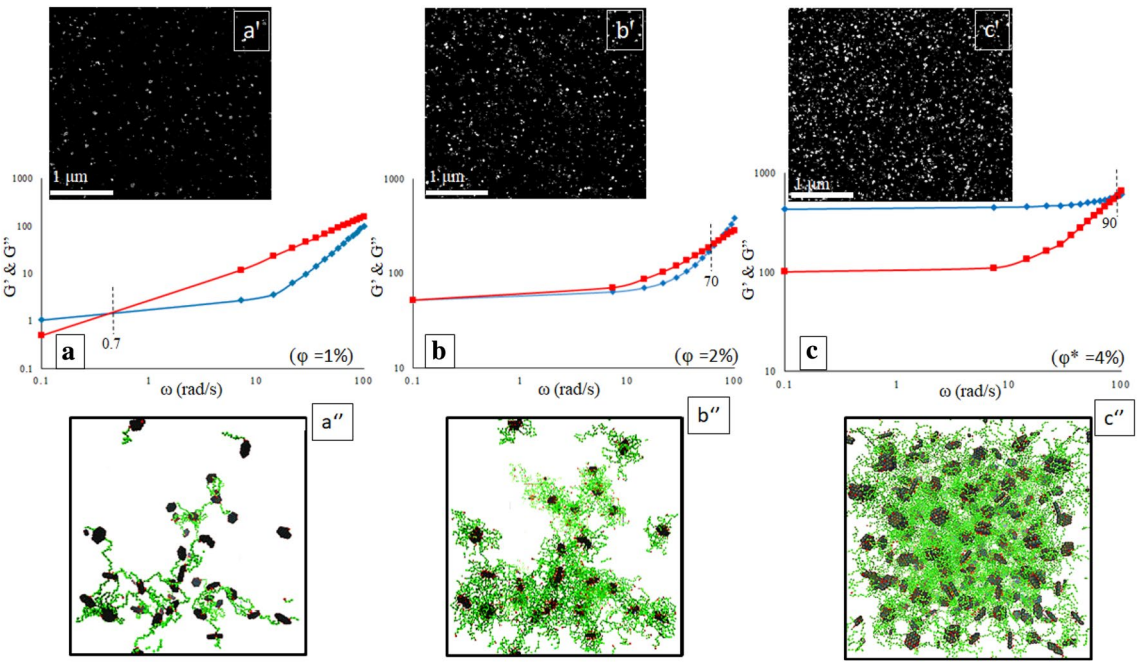

Fig. 4 **a**–**c** Storage modulus G′ (filled square) and loss modulus G″ (filled diamond) versus frequency of nanocomposite dispersion with 1, 2 and 4% of silica aerogel content, **a′**–**c′** SEM–EDX Si mapping images of silica aerogel in epoxy matrix with various wt%, **a″**–**c″** schematic illustration of percolation network formation with increasing silica aerogel content. With permission of Ref. [60]

organic–inorganic network was explained by Salimian et al. to describe the mesoporous silica aerogel-epoxy nanocomposite structure [36, 42].

3.3 Dynamic mechanical analysis (DMA)

The effect of mesoporous silica aerogel on the viscoelastic properties of crosslinked (cured) epoxy matrix nanocomposites has been explored with DMA performed from 40 to 180 °C. Figure 5 shows the temperature dependence of storage modulus (E′), and tan (δ) of the neat epoxy and silica aerogel-epoxy nanocomposites with different silica aerogel content. As shown in Fig. 5, the presence of the silica aerogel enhances the values of E′ with increasing silica aerogel content. Notably, a significant increase in E′ can be observed for nanocomposites with nanofiller content of φ*, showing approximately 2.5 magnitude increase for the nanocomposites over the pure epoxy in a transition region from glassy state to rubbery state (130 °C). When a polymer goes through the transition region, tan (δ) shows a maximum at the transition temperature (Tg), and a substantial drop in E′ appears, indicating viscous damping due to segmental motion of the main chains in the polymer. It is likely that this motion can be affected by nanofillers because of interactions in the interface between filler and matrix [62]. Moreover, Tg increases by around 12 °C at φ* and this indicates the chain mobility of the crosslinked epoxy is restricted due to mechanical anchoring of the epoxy polymer chains on the particle and the pore channels of the silica aerogel [63]. The increase in Tg is also confirmed by DSC and it display around 10 °C increment for nanocomposite containing 4% silica aerogel compared to neat epoxy which is in consistent with the DMA measurement (Fig. 5c). Obviously, the network structure which is formed at φ*, gives rise to better modulus reinforcement because the silica aerogel surrounded by an interface polymer layer act as large soft particles during the deformation process [36, 42].

3.4 Mechanical properties and fractography

The variations of mechanical properties consisting of flexural modulus and strength are demonstrated in Fig. 6. It can be seen that the characteristic mechanical properties of the epoxy nanocomposite are improved with various silica aerogel loadings which is a direct result of homogeneous dispersion of the filler within the matrix even at high filler contents. It is noteworthy that the flexural modulus and strength of the epoxy nanocomposite reach a maximum values with the mesoporous silica content at φ*, indicating ~ 40% and 80% improvement of mechanical strength and modulus respectively in comparison to neat epoxy. Owing to the high (meso)porosity, large surface area, pore size and pore volume of the silica aerogel, both the epoxy resin and the curing agent can readily penetrate into internal space of

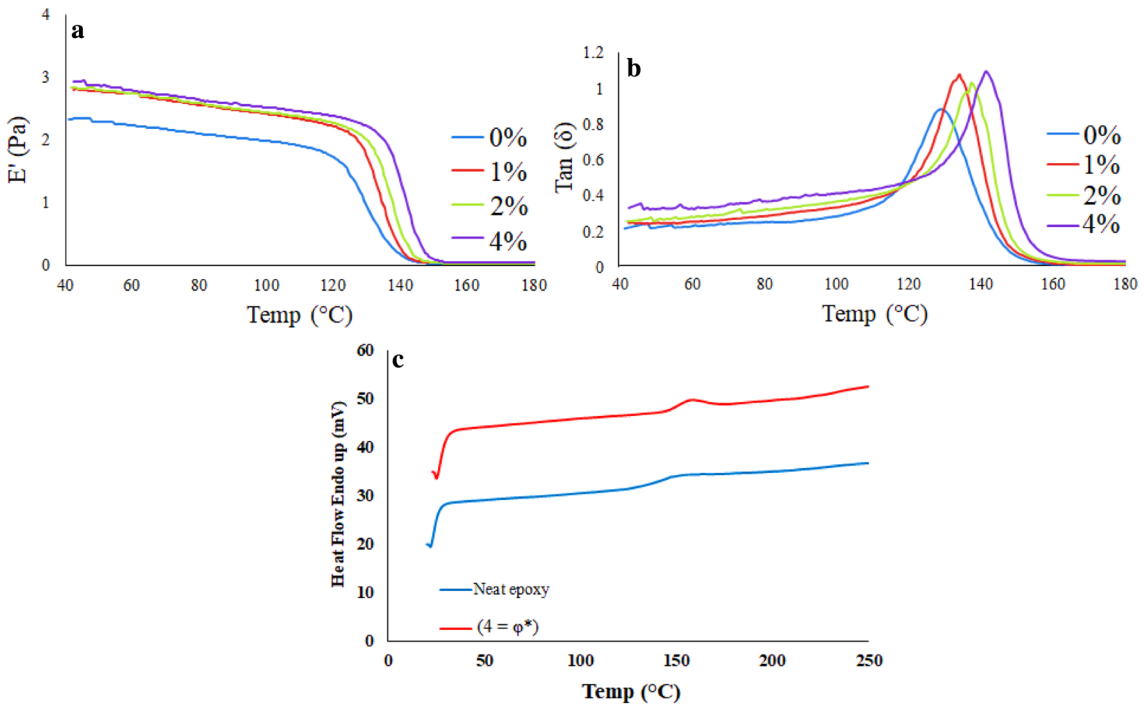

Fig. 5 The temperature dependence of **a** storage modulus (E′), and **b** tan (δ) of the neat epoxy as the reference and silica aerogel-epoxy nanocomposites with different silica aerogel content. **c** DSC of neat epoxy and the silica aerogel (4%)-epoxy nanocomposite

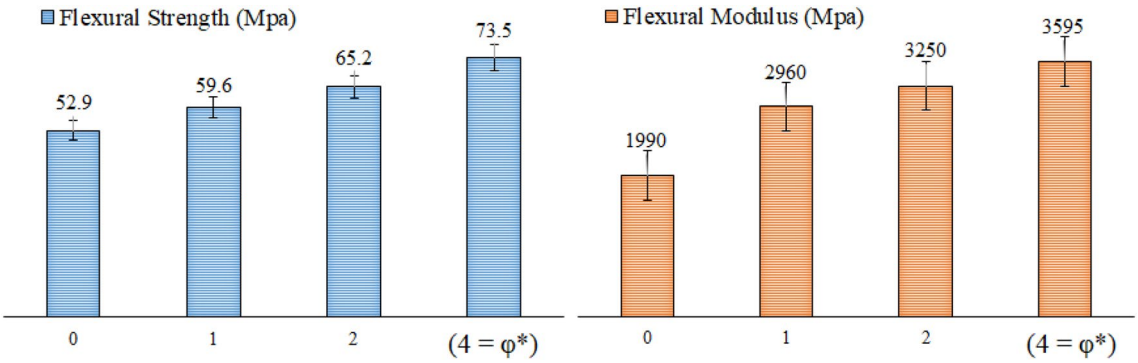

Fig. 6 Flexural **a** strength and **b** modulus of silica-aerogel epoxy nanocomposite at different silica aerogel content

mesoporous silica and form a nanocomposite with a unique structure and composition. The substantial improvements in the mechanical strength in mesoporous silica-epoxy nanocomposite has been reported before [64, 65]. In one of these studies, the increment of mechanical strength was attributed to the strong interfacial interactions and adhesion between the epoxy matrix and silica mesophase. It is important to note that favorable interfacial interactions are achieved in these nanocomposites without the need for organic modification of the silica surface. The high surface area of the mesoporous silica aerogel facilitates such interfacial interactions. Comparison between the results of flexural modulus and strength with those studied in the literature is presented in Table 1.

The strength of mesoporous silica-epoxy nanocomposites depend on the strength of the interface between the filler and the epoxy matrix and the micro-crack mechanism [70]. In particulate filled polymer systems, it is well known that the toughening effect of the filler arises due to crack deflection occurring when the crack front encounters the reinforcing particles, so the primary crack has to bend between the neighboring particles and passes between the silica–polymer interface and forming micro-cracks [71]. In order to analyze the possible existence of micro-crack and their influence on the mechanical properties in the present work, microscopic evaluations were conducted. The deformation mechanism of mesoporous silica aerogel-epoxy nanocomposites under flexural loading conditions are shown in Fig. 7. As shown in Fig. 7a crack pinning and deflection (bowing) can be clearly observed on the fracture surfaces of nanocomposite in flexural mode. In addition, the plastic void growth mechanism (debonding) is not identified which means that the separation between the interfaces is not occur and the crack propagates through the matrix around the mesoporous silica aerogel due to good interfacial adhesion between the filler and the matrix. The shear bands can be seen in Fig. 7b at higher magnification. This pattern is similar to shear bands in rubber modified epoxy systems [72], indicating that mesoporous particles have stiffening effect in this system and increase yield strength. When a shear stress is applied to such a system, the epoxy polymer engulfed between the mesophase spaces of silica aerogel undergoes shear deformation easier than that of the bulk of epoxy due to its higher entanglement density. Decrease in tendency to shear yield in nanocomposites may cause an increase in yield strength prior to fracture. Similar shear bands were observed for mesoporous silica aerogel–polymer nanocomposites [42, 73].

3.5 Silica aerogel–epoxy interface

The silica aerogels with nanoscale particles and a 3D-networked porous nanostructure are illustrated by TEM image (Fig. 8a) and the pores between the interconnected particles are also in nano-scale.

Table 1 Effect of different filler in the flexural modulus and strength of epoxy nanocomposite

Filler (in Epoxy matrix)	Weight (%)	Flexural strength (MPa)	Flexural modulus (MPa)	Author
Sodium silicate based silica aerogel	4	73.5	~3600	Salimian et al.
Silica aerogel-carbon nanotube	0.5	61.58	~2000	Mazlan et al. [66]
Mesoporous silica	5	109.1	~3400	Jiao et al. [67]
Silica nanoparticle	2	71.5	~2000	Kumar Singh et al. [68]
Nanoclay	1	110.35	~2700	Alsagayar et al. [69]

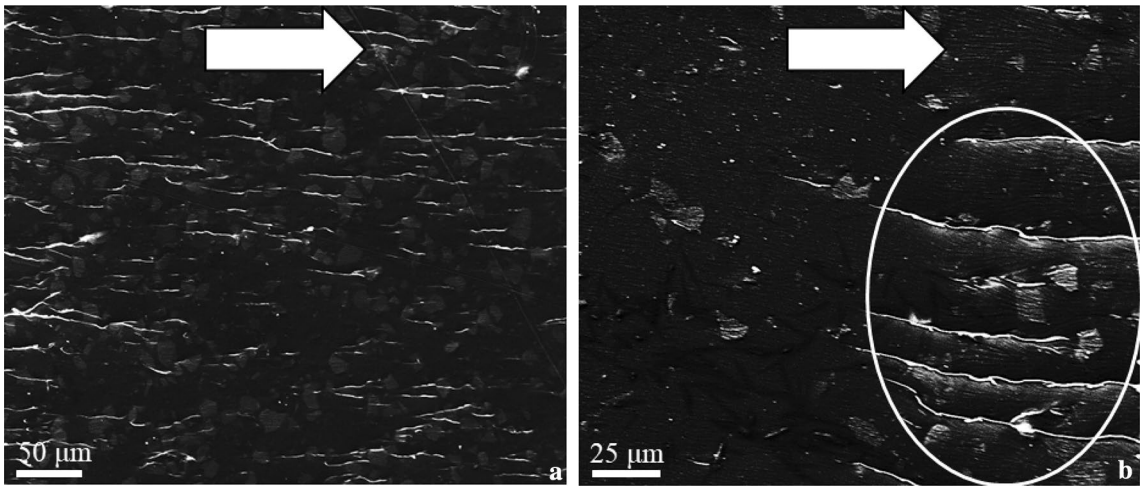

Fig. 7 Fracture surface of silica aerogel-epoxy at 4 wt% silica aerogel content observed under flexural loading. **a** Crack pinning and deflection and **b** shear bands formation mechanism (white circle). White arrows show the crack direction

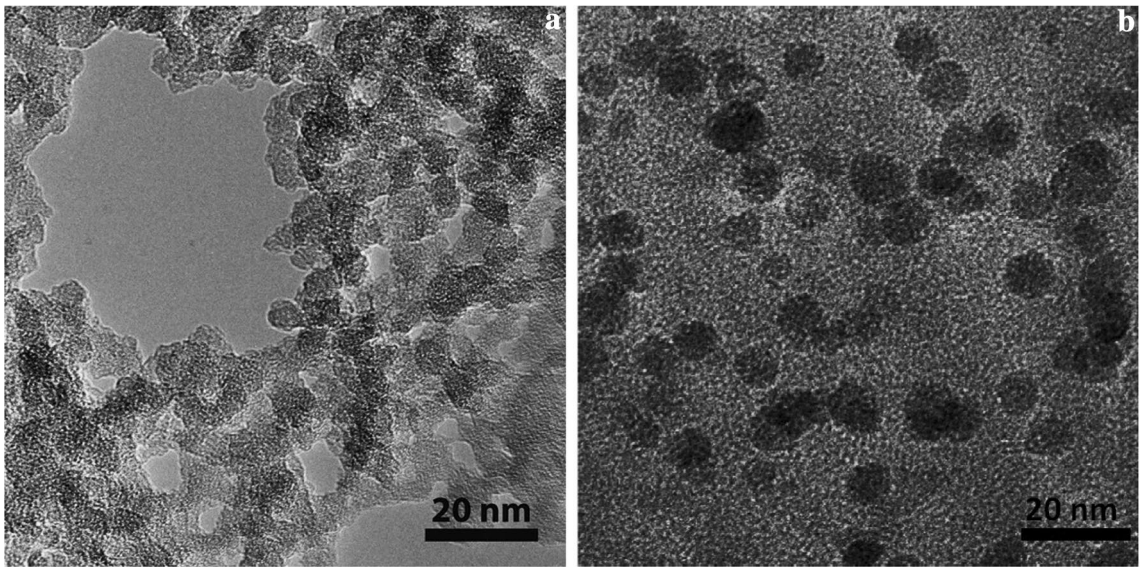

Fig. 8 **a** TEM image of silica aerogel structure and **b** secondary silica nanoparticles in epoxy phase matrix

TEM images in Fig. 8b are the nanomorphology of the composite showing the mesoporous silica nanoparticles dispersion states in composite. Nanopores of the silica aerogels have been totally infiltrated by epoxy to form silica nanoparticles-rich regions where the interconnected silica nanoparticles are dispersed homogeneously in the polymer matrix. Overall, in composites, silica nanoparticles keep their necklace-like shapes and spatial distribution patterns as in silica aerogels indicating that the mesoporous silica nanoparticles do not aggregate. The epoxy-impregnated aerogel phase is distributed evenly throughout the composite and the epoxy-filled aerogel phase itself can be considered as a high-quality dispersion of linked silica nanoparticles in which the epoxy was inserted into and totally occupied the nanopores. The TEM images confirm the formation of a nanocomposite with an interpenetrating organic–inorganic network structure [74]. The distribution states of silica nanoparticles in epoxy matrix affect the ability of composites to bear stress. Effectively connected silica nanoparticles help to disperse the loaded forces and improve the flexural modulus [75]. Importantly, voids and cracks are not visible at the interface between the particles and the epoxy. The large voids inside the composites cause the composite to be distorted and may be cracked when it exposed to high flexural stress.

4 Conclusion

In this study, we have used the water glass based silica aerogel as filler in epoxy system and have studied the rheological, mechanical and microstructural properties of dispersion and solid nanocomposite. On the basis of the rheological results, the microstructure of the dispersions changed at $\varphi^* \sim 4$ to form a percolation network structure. In general, a network structure which is formed at φ*, is proposed to play the main role in the reinforcement of nanocomposites. The interface polymer layer, surrounding and interpenetrating mesoporous silica particles, decreases the motion of the epoxy polymer and this results in an increase in Tg and E′. In addition, the mechanical properties (flexural modulus and strength) of the nanocomposite increases significantly at φ*, accounting for the dominant role of the interfacial adhesion between the filler and the matrix. The reason for the increase in mechanical strength originates in an influence of mesoporous silica aerogel on the structure and mobility of the polymer molecules.

Compliance with ethical standards

Conflict of interests The authors declare that they have no conflicts of interest.

References

1. Z.T. Mazraeh-shahi, A.M. Shoushtari, M. Abdouss, A.R. Bahramian, Relationship analysis of processing parameters with micro and macro structure of silica aerogel dried at ambient pressure. J. Non-Cryst. Solids **376**, 30–37 (2013)
2. Z. Mazrouei-Sebdani, S. Salimian, A. Khoddami, F. Shams-Ghahfarokhi, Sodium silicate based aerogel for absorbing oil from water: the impact of surface energy on the oil/water separation. Mater. Res. Express (2019). https://doi.org/10.1088/2053-1591/ab1eed
3. K.M. Saoud, S. Saeed, M.F. Bertino, L.S. White, Fabrication of strong and ultra-lightweight silica-based aerogel materials with tailored properties. J. Porous Mater. **25**, 511–520 (2018)
4. H. Maleki, L. Durães, A. Portugal, An overview on silica aerogels synthesis and different mechanical reinforcing strategies. J. Non-Cryst. Solids **385**, 55–74 (2014)
5. Z.T. Mazraeh-shahi, A.M. Shoushtari, A. Bahramian, A new approach for synthesizing the hybrid silica aerogels. Procedia Mater. Sci. **11**, 571–575 (2015)
6. Z. Mazrouei-Sebdani, A. Khoddami, H. Hadadzadeh, M. Zarrebini, A novel method to manufacture superhydrophobic and insulating polyester nanofibers via a meso-porous aerogel powder. *World Academy of Science, Engineering and Technology, International Journal of Chemical, Molecular, Nuclear, Materials and Metallurgical Engineering,* vol. 9, pp. 71–74
7. Z.T. Mazraeh-shahi, A.M. Shoushtari, A. Bahramian, A new method for measuring the thermal insulation properties of fibrous silica aerogel composite. Procedia Mater. Sci. **11**, 583–587 (2015)
8. Y. Zhang, F. Wang, P. Ou, H. Zhu, Y. Zhao, L. Wang et al., Prepared multifunctional aerogel for high performance supercapacitors and effective adsorbents. Mater. Res. Express **5**, 055508 (2018)
9. N. Hüsing, U. Schubert, Aerogels—airy materials: chemistry, structure, and properties. Angew. Chem. Int. Ed. **37**, 22–45 (1998)
10. Y. Duan, S.C. Jana, A.M. Reinsel, B. Lama, M.P. Espe, Surface modification and reinforcement of silica aerogels using polyhedral oligomeric silsesquioxanes. Langmuir **28**, 15362–15371 (2012)
11. Z.T. Mazraeh-Shahi, A.M. Shoushtari, A.R. Bahramian, M. Abdouss, Synthesis, pore structure and properties of polyurethane/silica hybrid aerogels dried at ambient pressure. J. Ind. Eng. Chem. **21**, 797–804 (2015)
12. X. Wang, S.C. Jana, Synergistic hybrid organic–inorganic aerogels. ACS Appl. Mater. Interfaces **5**, 6423–6429 (2013)
13. Z.T. Mazraeh-shahi, A.M. Shoushtari, A.R. Bahramian, M. Abdouss, Synthesis, structure and thermal protective behavior of silica aerogel/PET nonwoven fiber composite. Fibers Polym. **15**, 2154–2159 (2014)
14. L. Li, B. Yalcin, B.N. Nguyen, M.A.B. Meador, M. Cakmak, Flexible nanofiber-reinforced aerogel (xerogel) synthesis, manufacture, and characterization. ACS Appl. Mater. Interfaces **1**, 2491–2501 (2009)
15. A. Du, B. Zhou, Z. Zhang, J. Shen, A special material or a new state of matter: a review and reconsideration of the aerogel. Materials **6**, 941–968 (2013)
16. S. Salimian, A. Zadhoush, A. Mohammadi, A review on new mesostructured composite materials: Part I. synthesis of polymer-mesoporous silica nanocomposite. J. Reinf. Plast. Compos. **37**, 441–459 (2018)
17. A. Du, B. Zhou, Y. Li, X. Li, J. Ye, L. Li et al., Aerogel: a potential three-dimensional nanoporous filler for resins. J. Reinf. Plast. Compos. **30**, 912–921 (2011)
18. M. Rahmat, B. Ashrafi, A. Naftel, D. Djokic, Y. Martinez Rubi, M. Jakubinek et al., Enhanced shear performance of hybrid glass fibre-epoxy laminates modified with boron nitride nanotubes. ACS Appl. Nano Mater. (2018). https://doi.org/10.1021/acsanm.8b00413
19. F. Rahmani, S. Nouranian, Thermal analysis of montmorillonite/graphene double-layer coating as a potential lightning strike protective layer for crosslinked epoxy by molecular dynamics simulation. ACS Appl. Nano Mater. (2018). https://doi.org/10.1021/acsanm.8b00758
20. M. Naeimirad, A. Zadhoush, R.E. Neisiany, Fabrication and characterization of silicon carbide/epoxy nanocomposite using silicon carbide nanowhisker and nanoparticle reinforcements. J. Compos. Mater. **50**, 435–446 (2016)
21. S. Safi, A. Zadhoush, M. Ahmadi, Flexural and Charpy impact behaviour of epoxy/glass fabric treated by nano-SiO_2 and silane blend. Plast. Rubber Compos. **46**, 314–321 (2017)
22. A. Mohammadi, A. Valipouri, S. Salimian, Nanoparticle-loaded highly flexible fibrous structures exhibiting desirable thermoelectric properties. Diam. Relat. Mater. **86**, 54–62 (2018)
23. R.E. Neisiany, S.N. Khorasani, J.K.Y. Lee, M. Naeimirad, S. Ramakrishna, Interfacial toughening of carbon/epoxy composite by incorporating styrene acrylonitrile nanofibers. Theor. Appl. Fract. Mech. **95**, 242–247 (2018)
24. W. Li, J. Kong, T. Wu, L. Gao, Z. Ma, Y. Liu et al., Characterization, optical properties and laser ablation behavior of epoxy resin coatings reinforced with high reflectivity ceramic particles. Mater. Res. Express **5**, 046202 (2018)
25. S. Das, S. Halder, A. Sinha, M.A. Imam, N.I. Khan, Assessing nanoscratch behavior of epoxy nanocomposite toughened with silanized fullerene. ACS Appl. Nano Mater. **1**, 3653–3662 (2018)
26. Z. Raolison, C. Lefevre, J. Neige, A. Adenot-Engelvin, J. Greneche, N. Vukadinovic et al., Structural and microwave properties

of silica-coated NiFeMo flakes/polymer composites. Mater. Res. Express **2**, 026101 (2015)
27. S.S. Ray, M. Okamoto, Polymer/layered silicate nanocomposites: a review from preparation to processing. Prog. Polym. Sci. **28**, 1539–1641 (2003)
28. B. Li, P. I. Xidas, E. Manias, High breakdown strength polymer nanocomposites based on the synergy of nanofiller orientation and crystal orientation for insulation and dielectric applications. ACS Appl. Nano Mater. (2018)
29. S. Razavi, R.E. Neisiany, S.N. Khorasani, S. Ramakrishna, F. Berto, Effect of neat and reinforced polyacrylonitrile nanofibers incorporation on interlaminar fracture toughness of carbon/epoxy composite. Theor. Appl. Mech. Lett. **8**, 126–131 (2018)
30. S. Salimian, A. Zadhoush, A. Mohammadi, A review on new mesostructured composite materials: Part II. Characterization and properties of polymer–mesoporous silica nanocomposite. J. Reinf. Plast. Compos. **37**, 738–769 (2018)
31. M.A. Van Meer, B. Narasimhan, B.H. Shanks, S.K. Mallapragada, Effect of mesoporosity on thermal and mechanical properties of polystyrene/silica composites. ACS Appl. Mater. Interfaces **2**, 41–47 (2009)
32. Y. Chen, L. Wu, J. Zhu, Y. Shen, S. Gan, A. Chen, An organic/inorganic hybrid mesoporous silica membrane: preparation and characterization. J. Porous Mater. **18**, 251–258 (2011)
33. X. Ji, J.E. Hampsey, Q. Hu, J. He, Z. Yang, Y. Lu, Mesoporous silica-reinforced polymer nanocomposites. Chem. Mater. **15**, 3656–3662 (2003)
34. C. Amgoth, S. Joshi, Thermosensitive block copolymer [(PNIPAM)-b-(Glycine)] thin film as protective layer for drug loaded mesoporous silica nanoparticles. Mater. Res. Express **4**, 105306 (2017)
35. S. Salimian, A. Zadhoush, M. Naeimirad, R. Kotek, S. Ramakrishna, A review on aerogel: 3D nanoporous structured fillers in polymer based nanocomposites. Polym. Compos. **39**, 3383–3408 (2017)
36. S. Salimian, W.J. Malfait, A. Zadhoush, Z. Talebi, M. Naeimirad, Fabrication and evaluation of silica aerogel-epoxy nanocomposites: fracture and toughening mechanisms. Theor. Appl. Fract. Mech. **97**, 156–164 (2018). https://doi.org/10.1016/j.tafmec.2018.08.007
37. H. Najafi, A. Zadhoush, Z. Talebi, S.P. Rezazadeh Tehrani, Influence of porosity and aspect ratio of nanoparticles on the interface modification of glass/epoxy composites. Polym. Compos. **39**, 3073–3080 (2017)
38. J. P. Zhao, D. T. Ge, S. L. Zhang, and X. L. Wei, Studies on thermal property of silica aerogel/epoxy composite, in *Materials Science Forum*, 2007, pp. 1581–1584
39. N. Gupta, W. Ricci, Processing and compressive properties of aerogel/epoxy composites. J. Mater. Process. Technol. **198**, 178–182 (2008)
40. Z.A. Abdul Halim, M.A. Mat Yajid, M.H. Idris, H. Hamdan, Dispersion of polymeric-coated-silica aerogel particles in unsaturated polyester composites: effects on thermal-mechanical properties. J. Dispers. Sci. Technol. **39**, 1093–1101 (2018)
41. G.G. Kaya, E. Yilmaz, H. Deveci, Sustainable nanocomposites of epoxy and silica xerogel synthesized from corn stalk ash: enhanced thermal and acoustic insulation performance. Composite B **150**, 1–6 (2018)
42. S. Salimian, A. Zadhoush, Z. Talebi, B. Fischer, P. Winiger, F. Winnefeld et al., Silica aerogel-epoxy nanocomposites: understanding epoxy reinforcement in terms of aerogel surface chemistry and epoxy-silica interface compatibility. ACS Appl. Nano Mater. **1**, 4179–4189 (2018). https://doi.org/10.1021/acsanm.8b00941
43. T.-H. Hsieh, Y.-S. Huang, M.-Y. Shen, Mechanical properties and toughness of carbon aerogel/epoxy polymer composites. J. Mater. Sci. **50**, 3258–3266 (2015)
44. Z. Wang, X. Shen, M. Akbari Garakani, X. Lin, Y. Wu, X. Liu et al., Graphene aerogel/epoxy composites with exceptional anisotropic structure and properties. ACS Appl. Mater. Interfaces **7**, 5538–5549 (2015)
45. J. Tarrio-Saavedra, J. López-Beceiro, S. Naya, R. Artiaga, Effect of silica content on thermal stability of fumed silica/epoxy composites. Polym. Degrad. Stab. **93**, 2133–2137 (2008)
46. N. Suzuki, S. Kiba, Y. Yamauchi, Bimodal filler system consisting of mesoporous silica particles and silica nanoparticles toward efficient suppression of thermal expansion in silica/epoxy composites. J. Mater. Chem. **21**, 14941–14947 (2011)
47. J. Jiao, X. Sun, T.J. Pinnavaia, Mesostructured silica for the reinforcement and toughening of rubbery and glassy epoxy polymers. Polymer **50**, 983–989 (2009)
48. S. Kumar, S. Krishnan, S.K. Samal, S. Mohanty, S.K. Nayak, Toughening of petroleum based (DGEBA) epoxy resins with various renewable resources based flexible chains for high performance applications: a review. Ind. Eng. Chem. Res. **57**, 2711–2726 (2018)
49. Z. Mazrouei-Sebdani, A. Khoddami, H. Hadadzadeh, M. Zarrebini, Synthesis and performance evaluation of the aerogel-filled PET nanofiber assemblies prepared by electro-spinning. RSC Adv. **5**, 12830–12842 (2015)
50. ASTM D695-15, Standard Test Method for Compressive Properties of Rigid Plastics, ASTM International, West Conshohocken, PA, www.astm.org (2015)
51. ASTM D790-17, Standard Test Methods for Flexural Properties of Unreinforced and Reinforced Plastics and Electrical Insulating Materials, ASTM International, West Conshohocken, PA, www.astm.org (2017)
52. Y. Duan, S.C. Jana, B. Lama, M.P. Espe, Reinforcement of silica aerogels using silane-end-capped polyurethanes. Langmuir **29**, 6156–6165 (2013)
53. O. van den Berg, J.R. Capadona, C. Weder, Preparation of homogeneous dispersions of tunicate cellulose whiskers in organic solvents. Biomacromol **8**, 1353–1357 (2007)
54. N.A. Dudukovic, L.L. Wong, D.T. Nguyen, J.F. Destino, T.D. Yee, F.J. Ryerson et al., Predicting nanoparticle suspension viscoelasticity for multimaterial 3D printing of silica-titania glass. ACS Appl. Nano Mater. **1**, 4038–4044 (2018)
55. T.-X. Lin, K.-J. Chen, P.-Y. Chen, J.-S. Jan, Broadband antireflection coatings based on low surface energy/refractive index silica/fluorinated polymer nanocomposites. ACS Appl. Nano Mater. **1**, 741–750 (2018)
56. D. Ge, L. Yang, Y. Li, J. Zhao, Hydrophobic and thermal insulation properties of silica aerogel/epoxy composite. J. Non-Cryst. Solids **355**, 2610–2615 (2009)
57. J.M. Allan, M.A. Mumin, J.A. Wood, W.Z. Xu, W. Wu, P.A. Charpentier, Silica aerogel–poly (ethylene-co-vinyl acetate) composite for transparent heat retention films. J. Polym. Sci. B **52**, 927–935 (2014)
58. A.C. Pierre, G.M. Pajonk, Chemistry of aerogels and their applications. Chem. Rev. **102**, 4243–4266 (2002)
59. J. Zhu, S. Wei, A. Yadav, Z. Guo, Rheological behaviors and electrical conductivity of epoxy resin nanocomposites suspended with in situ stabilized carbon nanofibers. Polymer **51**, 2643–2651 (2010)
60. D. Xu, D. Gersappe, Structure formation in nanocomposite hydrogels. Soft Matter **13**, 1853–1861 (2017)
61. R. Kotsilkova, D. Fragiadakis, P. Pissis, Reinforcement effect of carbon nanofillers in an epoxy resin system: rheology, molecular dynamics, and mechanical studies. J. Polym. Sci. B **43**, 522–533 (2005)

62. A.K. Yadav, S. Banerjee, R. Kumar, K.K. Kar, J. Ramkumar, K. Dasgupta, Mechanical analysis of nickel particle-coated carbon fiber-reinforced epoxy composites for advanced structural applications. ACS Appl. Nano Mater. **1**(8), 4332–4339 (2018)
63. C.-F. Cheng, H.-H. Cheng, P.-W. Cheng, Y.-J. Lee, Effect of reactive channel functional groups and nanoporosity of nanoscale mesoporous silica on properties of polyimide composite. Macromolecules **39**, 7583–7590 (2006)
64. I. Park, H.-G. Peng, D.W. Gidley, S. Xue, T.J. Pinnavaia, Epoxy–silica mesocomposites with enhanced tensile properties and oxygen permeability. Chem. Mater. **18**, 650–656 (2006)
65. J. Lin, X. Wang, Preparation, microstructure, and properties of novel low-κ brominated epoxy/mesoporous silica composites. Eur. Polym. J. **44**, 1414–1427 (2008)
66. N. Mazlan, N. Termazi, S. Abdul Rashid, S. Rahmanian, Investigations on composite flexural behaviour with inclusion of CNT enhanced silica aerogel in epoxy nanocomposites, in *Applied Mechanics and Materials*, pp. 179–182 (2015)
67. J. Jiao, L. Wang, P. Lv, Y. Cui, J. Miao, Improved dielectric and mechanical properties of silica/epoxy resin nanocomposites prepared with a novel organic–inorganic hybrid mesoporous silica: POSS–MPS. Mater. Lett. **129**, 16–19 (2014)
68. S.K. Singh, A. Kumar, A. Jain, Improving tensile and flexural properties of SiO_2–epoxy polymer nanocomposite. Mater. Today **5**, 6339–6344 (2018)
69. Z. S. Alsagayar, A. R. Rahmat, and A. Arsad, Tensile and flexural properties of montmorillonite nanoclay reinforced epoxy resin composites, in *Advanced Materials Research*, pp. 373–376 (2015)
70. M. Naeimirad, A. Zadhoush, R.E. Neisiany, S. Ramakrishna, S. Salimian, A.A. Leal, Influence of microfluidic flow rates on the propagation of nano/microcracks in liquid core and hollow fibers. Theor. Appl. Fract. Mech. **96**, 83–89 (2018)
71. Q. Zhao, S. Hoa, Toughening mechanism of epoxy resins with micro/nano particles. J. Compos. Mater. **41**, 201–219 (2007)
72. J. Parameswaranpillai, S.K. Sidhardhan, S. Jose, N. Hameed, N.V. Salim, S. Siengchin et al., Miscibility, phase morphology, thermomechanical, viscoelastic and surface properties of poly (ε-caprolactone) modified epoxy systems: effect of curing agents. Ind. Eng. Chem. Res. **55**, 10055–10064 (2016)
73. I. Lázár, H.F. Bereczki, S. Manó, L. Daróczi, G. Deák, I. Fábián et al., Synthesis and study of new functionalized silica aerogel poly (methyl methacrylate) composites for biomedical use. Polym. Compos. **36**, 348–358 (2015)
74. M. Run, S. Wu, D.Y. Zhang, G. Wu, A polymer/mesoporous molecular sieve composite: preparation, structure and properties. Mater. Chem. Phys. **105**, 341–347 (2007)
75. Y. Li, L. Dong, X. Zhang, Y. Lu, W. Fang, Y. Yang, Preparation of carbon nanotubes/epoxy composites using novel aerogel substrates. Mater. Lett. **160**, 432–435 (2015)